

Development of a Compartmental Model of Zinc Kinetics in Mice^{1,2}

Meryl E. Wastney^{3*} and William A. House⁴

³Metabolic Modeling Services, 7201 Blenheim, New Zealand and ⁴USDA-Agricultural Research Service, Robert W. Holley Center for Agriculture and Health, Ithaca, NY 14853

Abstract

To investigate zinc (Zn) kinetics in mice, tracer (⁶⁵Zn) was administered orally to 9-wk-old female mice in the fed state and tracer and Zn concentration were measured in 21 tissues over the following 8 d. Data were analyzed by compartmental modeling using WinSAAM. A published model for Zn kinetics in rats was modified to fit the data from mice and to calculate transfer rates and pool sizes of Zn. Parallel studies were performed in mice lacking genes for metallothionein (MT), MT-I and MT-II (MT^{-/-}), to quantify differences in Zn kinetics in the absence of these proteins *in vivo*. We confirmed that tracer time course in most tissues was similar in wild-type mice and those lacking MT, except for the pancreas of MT^{-/-}, which retained less tracer. By fitting tissue and intestinal data simultaneously, we found that intestinal tracer could be explained by unabsorbed isotope and loss of Zn from pancreas went through plasma. Differences in pancreatic data in MT^{-/-} were explained by Zn turning over twice as fast in this tissue (4 h) compared with wild type (9 h). These kinetic studies provide parameter values for normal, fed mice that can be used to assess Zn kinetics in abnormal conditions, as demonstrated by the higher turnover of Zn in the pancreas of MT knockout mice. *J. Nutr.* 138: 2148–2155, 2008.

Introduction

Compartmental models provide quantitative values for metabolism such as transport rates and pool sizes (1,2). Detailed models have been published for zinc (Zn) metabolism in humans (3–5), rats (1,6), and piglets (7) but not for mice, even though their Zn kinetics have been studied extensively (8–11). Because mice are being used to study biological functions of proteins by knocking out or overexpressing genes, kinetic studies in genetically modified mice, combined with modeling, may provide insight into their functions *in vivo*.

Many biological functions of Zn are associated with proteins (12) and there has been an explosion of information concerning proteins involved in Zn uptake and release by cells via Zn transporters (13–15), as well as the storage of Zn within cells by metallothionein (MT)⁵ (16,17). Two major isoforms of this protein, MT-I and MT-II, assimilate Zn in tissues in rodents (18,19). Although the genes are induced by a number of factors, including hormones, stress, and administration of metals (20), mice lacking gene expression for MT-I and MT-II appear to grow and reproduce normally (21,22) and the physiological role of MT

remains unclear (23,24), although it appears to be important during times of stress (25).

Possible roles for MT in Zn metabolism have been explored with tracer studies in MT-knockout mice (26,27). Following subcutaneous administration of Zn tracer, low levels (1–2%) of tracer were detected in the small intestine and it was concluded that an absence of MT in the pancreas contributed to more Zn secretion in exocrine secretions. Studies on the mice used, however, have been questioned (23), because the control and knockout mice may not have had identical genetic backgrounds. The pancreas has one of the highest concentrations of MT (28,29) and because *in vitro* (30) and *in vivo* studies (31) indicate that MT can accept and donate Zn, MT may have a role in exocrine functions by regulating or modulating Zn utilization.

The aim of the current study was to develop a multi-compartmental model for Zn kinetics in mice by administering tracer and sampling multiple tissues over several days. The objectives were to provide baseline values for Zn kinetics in mice under replete dietary conditions and to then quantify differences in Zn metabolism between normal mice and those lacking MT.

Experimental Procedures

Mice and diet. Young, 9-wk-old, female mice were used to assess Zn kinetics. Mice were purchased (Jackson Laboratory)⁶ when they were 7 wk of age. Mice (strain 129/Sv-+ < *P* > +

¹ Supported in part by NIH grant DK53787. The costs of publication of this article were defrayed in part by payment of page charges. This article must therefore be hereby marked "advertisement" in accordance with 18 U.S.C. Section 1734 solely to indicate this fact.

² Author disclosures: W. A. House and M. E. Wastney, no conflicts of interest.

⁵ Abbreviations used: MT, metallothionein; MT^{-/-}, MT-null or mice lacking metallothionein isoforms I and II; WT, wild-type or mice with metallothionein isoforms I and II.

* To whom correspondence should be addressed. E-mail: wastneym@metabolic-modeling-services.com.

⁶ Mention of a trade name or a proprietary product does not constitute a guarantee or warranty of the product by USDA or imply its approval to the exclusion of other products or vendors that may be suitable.

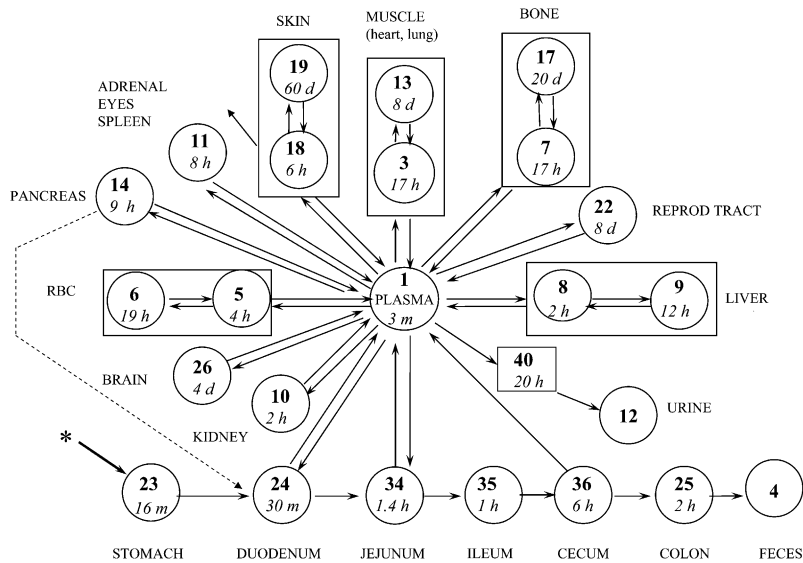


FIGURE 1 Model for Zn metabolism in mice consists of compartments (circles) and transfer pathways (arrows). Compartment numbers (in bold) are: 1, plasma; 5 and 6, RBC; 3 and 13, muscle; 7 and 17, bone; 8 and 9, liver; 10, kidney; 11, includes spleen, adrenals, and eyes; 14, pancreas; 18 and 19, skin; 22, part of reproductive tract; 26, brain; 23, stomach; 24, duodenum; 34, jejunum; 35, ileum; 36, cecum; and 25, colon. The intestinal compartments are assumed to represent Zn in the lumen and additional exchange compartments (not shown) were added for Zn in intestinal tissue. Heart and lung were fitted as a fraction of compartment 3. Zn was assumed to leave the system via urine (compartment 12) after a 20-h delay (compartment 40), feces (compartment 4), and because of hair shedding and epidermal desquamation (skin, compartment 18). The asterisk indicates the site of tracer administration, per os. Smaller number in circles indicates the turnover time of each compartment in min (m), h, or d. The dotted line indicates an alternative pathway to L(34,1) for endogenous fecal excretion of Zn. Turnover of Zn in the pancreas was faster (4 h) for MT-null mice than for WT mice (9 h).

< Tyr-c > + < Mgf-S1J > /J, designated 129/Sv) ($n = 43$) were placed in individual stainless steel metabolism cages in a room maintained at 22°C and 45% relative humidity with a 12-h-light/dark cycle. All mice were fed a commercially prepared (Dyets) egg white-based diet, modified slightly from the AIN-93G (32) formulation, which contained 101 mg Zn/kg diet. The mice had free access to feed and deionized water during both a 14-d adjustment period and an 8-d experimental period. Animal care procedures followed NIH and USDA guidelines and were approved by the Institutional Animal Care and Use Committee at Cornell University, Ithaca, NY. Parallel studies were performed in MT-null mice (strain 129/Sv-Mt1Mt2 < tm1Bri >) ($n = 47$) that did not express MT-I and MT-II proteins. The MT status of the mice was verified by determining the MT content of the stomach mucosa. Tissues from 4 mice of each genotype were prepared and analyzed for MT using a cadmium-binding assay (33).

In separate groups of mice, aged 9 or 34 wk, 15 mice of each genotype were food deprived for 12–14 h, anesthetized, and a blood sample was obtained from the tail. A glucometer (FastTake, LifeScan) was used to determine blood glucose concentration. A radioimmunoassay kit (no. SRI-13K, Linco Research) was used to measure insulin in small samples of plasma (~20 μ L).

Isotope administration and sampling. Non-food-deprived mice were given by oral gavage 18.5 kBq (0.5 μ Ci) of $^{65}\text{ZnCl}_2$ (DuPont de Nemours; 88.5 mBq/ μ g Zn) in 0.1 mL of deionized water. Immediately after ^{65}Zn was given, some mice were assayed for radioactivity in a custom-built “whole-body” gamma scintillation spectrometer described previously (34). Subsequently, mice were assayed and whole-body retention of ^{65}Zn was measured daily until the mice were killed. At 10 time points after isotope administration (0.5, 1, 2, 3, 6, 12, 24, 48, 96, and 192 h), 3–5 mice of each strain were anesthetized and blood was collected by cardiac puncture into heparinized tubes. These mice were then killed by CO_2 anesthesia and dissected to obtain organs and tissue samples. Daily food consumption was measured and urine and feces were collected separately each day on the mice killed at 96 and 192 h (8–10 mice per strain).

Blood samples were centrifuged and plasma and formed elements were separated. The entire liver, kidneys, adrenal

glands, spleen, heart, lungs, pancreas, brain, eyes, reproductive tract, and gastrointestinal tract were removed from each mouse. Additionally, the pelt, samples of bone (femur), and skeletal muscle were collected from each mouse; the pelt, which included the ears, was removed as nearly as completely as possible. The gastrointestinal tract was divided into the following anatomical segments: stomach, duodenum (proximal 8 cm of small intestine), jejunum (mid-region of small intestine), ileum (distal 8 cm of small intestine), cecum, and colon. The reproductive tract included the vagina, left and right uterine horns, oviducts and ovaries; fat and supporting mesentery were removed. All remaining parts of the carcass were pooled and saved.

Zn and ^{65}Zn analysis. Tissues, organs, excreta, and intestinal segments (with contents) from each mouse were assayed for ^{65}Zn activity by a scintillation detector (Model 5530, Packard Instrument) and activity was expressed as a percentage of the oral dose. Tissues were then saved to determine total Zn content. Prior to chemical analysis, each intestinal segment was slit open along its horizontal axis and digesta removed by flushing with cold physiological saline. Organs, tissues, excreta, and diet samples were dried (70°C for 48–96 h), wet-digested in a mixture of

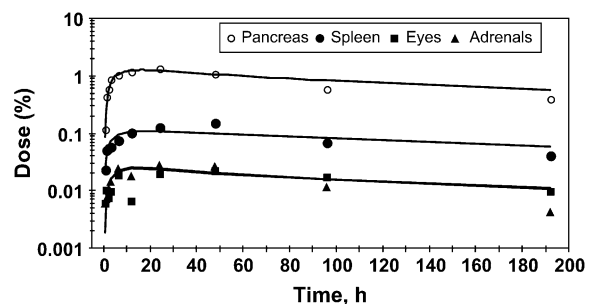


FIGURE 2 Tracer appearance in pancreas, spleen, eyes, and adrenals of mice after oral administration of ^{65}Zn ; the similar patterns indicate that the kinetics are alike. Values are means, $n = 3$ –5 mice. The curves were calculated using the model in Figure 1 and parameter values in Table 4.

HNO₃ and HClO₄ (9:1, v:v), and analyzed for Zn using inductively coupled plasma emission spectrometry (Trace Analyzer, Thermo Jarrell Ash). For all analyses, minerals measured in a standard reference material (no. 1577b, bovine liver, National Institute of Standards and Technology) were within certified ranges.

The total amount of ⁶⁵Zn and Zn in whole organs or tissues was calculated from the ⁶⁵Zn and Zn content of the samples combined with the measured or estimated weights of the organs. Literature values (6,29) were used to estimate volumes of plasma and RBC, and total weight and dry matter content of bone and muscle. Values used, expressed as a percentage of body weight, were: plasma, 2.1%; RBC, 3.2%; bone, 11.2%; and muscle, 38.8%. The ⁶⁵Zn tracer data for each of the 21 tissues collected at each sampling time were expressed as a percentage of the amount administered.

Kinetic analysis. Changes in ⁶⁵Zn distribution in the body were analyzed using compartmental analysis and the modeling software WinSAAM (35,36). Kinetic terms and symbols were as reported previously (1). Briefly, compartments represented pools of Zn in the body. The pools may represent Zn in different tissues or metabolic forms that differ kinetically. Transfer between compartments, $L(i,j)$, was the fraction transferred per hour into compartment i from compartment j . $M(i)$ represented Zn mass (μg) [Zn molecular weight is 65.4] in compartment i .

Statistics. Values were expressed as means \pm SEM. Group means for the Zn and radiozinc data were compared using Student's t test. Similarly, blood glucose and plasma insulin concentrations were compared using a t -test procedure. Differences were considered significant at $P < 0.05$; actual P -values < 0.1 are reported.

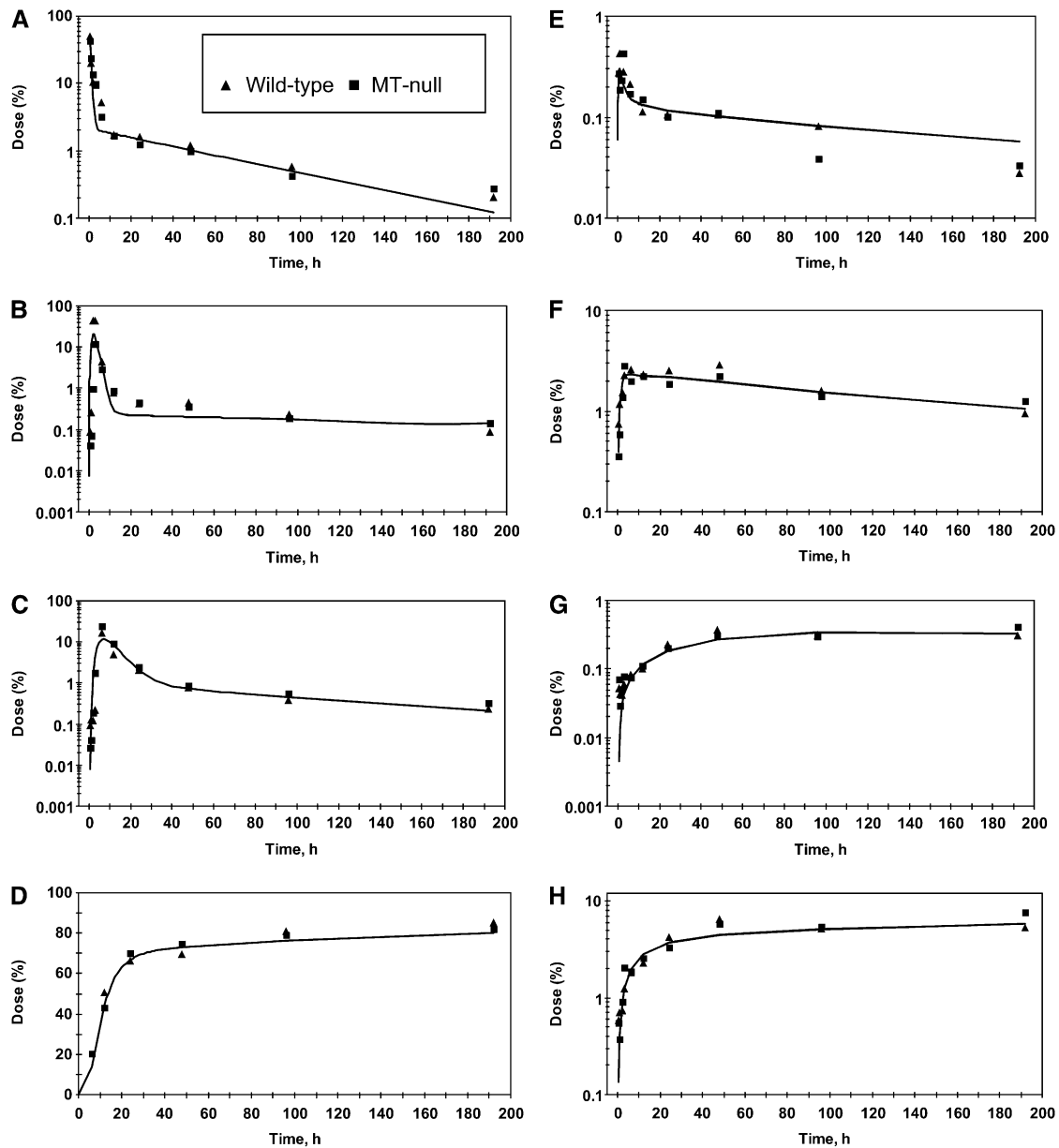


FIGURE 3 Time course of tracer in some tissues and feces of WT and MT-null mice after oral administration of ⁶⁵Zn. Intestinal segments (tissue and luminal contents) are the duodenum (A), ileum (B), colon (C), and feces (D). Other tissues are plasma (E), liver (F), brain (G), and bone (H). Each point is the mean of 3–5 mice. The curves were calculated using the model in Figure 1 and parameter values in Table 4.

Model Fitting and Results

Control, wild-type mice. The ^{65}Zn data for the female mice were fitted initially using a compartmental model of Zn metabolism developed for male rats (1). The model was extended to fit data from the additional tissues sampled in this study and modified to fit Zn kinetics in the mouse. The rate constants in the mouse model were adjusted to obtain a best fit to the data as indicated by obtaining a minimal residual sum of squares for error between observed and model-calculated values. To facilitate comparisons between species, numbers used to identify the different compartments in the mouse model were the same as those used in the rat (1) and human (4) models. Assumptions in the model were that: 1) absorption occurred from multiple sites in the intestine; 2) endogenous intestinal secretion occurred from plasma into 2 sites (the duodenum and jejunum); and 3) absorption of exogenous tracer and endogenously secreted tracer was similar. The model for Zn kinetics in mice (Fig. 1) consists of compartments representing plasma, RBC, muscle, bone, liver, kidney, spleen, skin, duodenum, jejunum, ileum, cecum, and colon and other tissues. Zn was lost from the system through urine, feces, and skin because of hair shedding and epidermal desquamation. Appearance of tracer in urine occurred after a delay of 20 h. Data from the female reproductive tract was fitted using fractions of compartment 22 (1.5%) and compartment 3 (10%). A compartment, number 26, was added to fit brain data. The tracer kinetics in eyes and adrenals were similar to those of the spleen (Fig. 2) and all 3 were fitted as portions (0.3, 0.3, and 1.1%, respectively) of compartment 11. The pancreas had similar kinetics to these tissues (Fig. 2), but compartment 14 was added to represent the pancreas because pancreatic kinetics differed between genotypes (described below). The heart and lung data were both fitted by using a portion (6 and 11%, respectively) of the pool of Zn in muscle (compartment 3, Fig. 1) that had the faster rate of turnover. Compartment 23 was added to fit the stomach data. Separate compartments (not shown on the figure for clarity) were added (compartments 21, 33, 37, 39, 41, and 42) to exchange with the stomach, duodenum, jejunum, ileum, cecum, and colon, respectively. These were required to fit the tracer data and probably represent Zn in the gut tissues, whereas compartments 23–25 and 34–36 probably represent tracer in the intestinal lumen. Turnover of Zn in the intestinal exchange compartments was slow (~ 10 d). Secretion pathways from plasma into the intestine, defined following i.v. tracer administration in rats (1), were retained in the mouse model. Summing all compartments (excluding urine and feces) fit the whole-body data. As described for rats, exchange with compartments in skin and muscle that turned over slowly, and not defined from these 8-d studies, was fixed by the measured Zn mass in the tissue (1). Absorption was calculated as the fraction of tracer entering plasma from each site in the intestine (compartments 24, 34, and 36) and the fractions were added to determine total absorption. For example, absorption from the duodenum was calculated as $L(1,24)/(L(1,24)+L(34,24))$. Absorption capacity from each was: duodenum, 3.8%; jejunum, 12.5%; and cecum, 9%. Based on the percent of dose arriving at each site, this translated into 4, 12, and 7% absorption, respectively, of the orally administered ^{65}Zn dose for a total absorption of 23%. The time courses of tracer appearance in some tissues (Fig. 3) were compared with values calculated by the model (Fig. 1) of Zn metabolism in the mice.

MT-/- mice. Concentrations of MT in the stomach mucosa of wild-type (WT) and MT-/- mice were 12.7 ± 2.1 and 1.8 ± 0.2 nmol cadmium bound/g wet weight, respectively. As

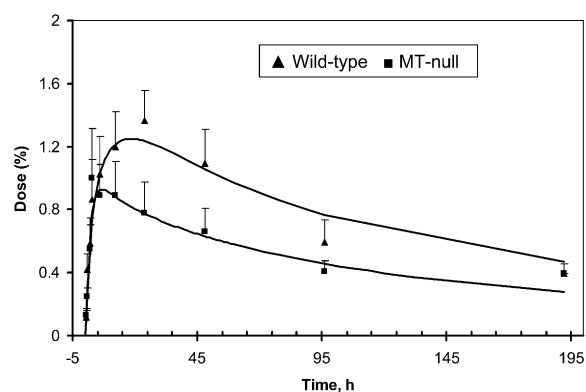


FIGURE 4 Tracer appearance in pancreas of WT and MT-null mice (mean \pm SEM, $n = 3$ –5) after oral administration of ^{65}Zn .

reported by others (19), the values for the MT-null mice were assumed to represent nonspecific cadmium binding and not MT.

The body weight of MT-/- mice was greater than that of WT mice (Table 1). Blood glucose and plasma insulin concentrations were 20 and 27% higher, respectively, in MT-null mice than in the WT mice (Table 1). Following intraperitoneal glucose administration, glucose disappearance and insulin kinetics did not differ over time (data not shown). In 34-wk-old mice, differences between genotypes in fasting glucose ($P = 0.065$) and insulin ($P = 0.086$) were not significant and glucose tolerance did not differ (data not shown).

Concentrations of Zn in many tissues were lower in MT-/- mice than in WT mice (Table 2); generally, differences between genotypes were $\sim 10\%$. However, the amount and concentration of Zn in the pancreas differed more markedly between genotypes. The total amount of Zn in most tissues did not differ between genotypes, but in some tissues (brain, kidney, lung, pancreas, and reproductive tract), Zn content was lower in MT-null mice than in WT mice (Table 3). Muscle, by contrast, had higher total Zn mass in MT-/- than in WT mice. The Zn mass observed in each tissue was compared with the value calculated using the model and predictions were within 30% for most tissues (Table 3).

In most tissues, tracer values did not differ between WT and MT-/- mice. However, the amount of ^{65}Zn in the pancreas was

TABLE 1 Characteristics of WT and MT-null (MT-/-) mice studied¹

Item ²	Genotype	
	WT (n)	MT-/- (n)
Body weight, g	19.8 \pm 0.3 (43)	20.7 \pm 0.3 (47)*
Zn intake, $\mu\text{g}/\text{d}^3$	261 \pm 10 (8)	273 \pm 6 (9)
Plasma Zn, $\mu\text{g}/\text{g wet wt}$	1.71 \pm 0.09 (43)	1.82 \pm 0.04 (47)
RBC Zn, $\mu\text{g}/\text{g wet wt}$	8.60 \pm 0.43 (43)	8.26 \pm 0.26 (47)
Urine Zn, $\mu\text{g}/\text{d}$	1.4 \pm 0.1 (8)	1.5 \pm 0.1 (9)
Fecal Zn, $\mu\text{g}/\text{d}$	242 \pm 15 (8)	223 \pm 3 (9)
Blood glucose, $\mu\text{mol}/\text{L}$	3.61 \pm 0.11 (15)	4.33 \pm 0.28 (15)*
Plasma insulin, pmol/L	37.9 \pm 3.4 (8)	48.2 \pm 3.4 (8)*

¹ Values are means \pm SEM. *Different from wild-type, $P < 0.05$.

² Body weight, plasma Zn, and RBC Zn were measured in all mice whereas Zn intake, urine, and fecal Zn were measured only in mice studied for >96 h. Blood glucose and plasma insulin concentration were measured in a separate group of mice that were anesthetized after a 12-h food deprivation.

³ To convert to $\mu\text{mol}/\text{g}$, multiply by 0.0153.

TABLE 2 Zn concentrations in tissues of WT and MT-null (MT^{-/-}) mice¹

Tissue	Genotype		Difference
	WT, n = 43	MT ^{-/-} , n = 47	
	$\mu\text{g/g dry weight}^2$		%
Adrenal gland	32 ± 2	30 ± 2	-6
Bone	203 ± 4	201 ± 1	-1
Brain	72 ± 1	66 ± 1**	-8
Cecum	288 ± 24	257 ± 22	-11
Colon	148 ± 8	167 ± 12	13
Duodenum	119 ± 2	114 ± 3	-4
Eye	39 ± 2	36 ± 3	-7
Heart	72 ± 1	69 ± 1**	-4
Ileum	191 ± 14	170 ± 13	-11
Jejunum	140 ± 5	160 ± 6*	14
Kidney	75 ± 1	68 ± 1**	-10
Liver	87 ± 1	78 ± 1**	-10
Lung	74 ± 2	66 ± 1**	-11
Muscle	38 ± 1	36 ± 1	-4
Pancreas	133 ± 2	105 ± 2*	-21
Pelt	58 ± 2	54 ± 2*	-8
Reproductive tract	59 ± 2	52 ± 2*	-11
Spleen	89 ± 3	77 ± 2**	-14
Stomach	81 ± 6	81 ± 7	0

¹ Values are means ± SEM. *Different from WT, $P < 0.05$; ** $P < 0.01$.

² To convert to $\mu\text{mol/g}$, multiply by 0.0153.

lower in MT^{-/-} mice than in the WT mice (Fig. 4). The latter difference between genotypes was apparent by 10 h after tracer administration and the difference persisted for up to 8 d. Pancreas data from MT^{-/-} were fitted by doubling the loss of Zn from the pancreas [L(1,14); Fig. 1] in MT^{-/-} (0.24/h) compared with WT mice (0.11/h; Table 4). Turnover time of Zn in pancreas [calculated as 1/L(1,14)] was 9 h in WT and 4 h in MT^{-/-}. We performed a test to determine whether the loss pathway from the pancreas to plasma could be replaced by a loss to the duodenum [i.e. L(24,14) vs. L(1,14); Fig. 1], but the model fit to the data was poorer. Yet, the model could fit the data if a pancreas-to-duodenal loss pathway was added in place of the plasma-jejunum pathway [L(34,1); Fig. 1]. With this variation, loss from the pancreas to duodenum was similar between genotypes (0.03/h), whereas loss from the pancreas to plasma was >2-fold higher in MT^{-/-} (0.22/h) than in WT (0.08/h). Because the loss to plasma appeared to be the predominant route of Zn loss from pancreas, we retained the version of the model with the L(1,14) pathway. All other parameter values were similar for both genotypes. Moreover, Zn absorption by the MT-null mice (23%) was the same as for the WT mice.

Discussion

Zn kinetics in mice vs. rats and humans

WT mice. This study provides basal values for Zn kinetics in normal, nutritionally replete female mice, which allows comparison to mice with differing dietary, genetic, or physiological conditions. The kinetic data agree with those of Sheline et al. (8) in that the relative turnover of Zn: 1) was most rapid in liver, pancreas, and kidney; 2) was the slowest in RBC, brain, skeletal muscle, and skin; and 3) was intermediate in spleen, gastrointestinal tract, adrenals, lungs, bone, heart, and thymus. Here we quantified the turnover rates and showed that some tissues (skin, muscle, and bone) contain both rapidly and slowly turning-over

TABLE 3 Mass of Zn in tissues of WT and MT-null (MT^{-/-}) mice by measurement and calculation by the model¹

	Genotype			
	WT		MT ^{-/-}	
	μg^2	C:O ratio ³	μg	C:O ratio ³
Adrenals	0.133 ± 0.004	1.55	0.170 ± 0.017	1.36
Bone	281.6 ± 10.3	0.83	292.7 ± 6.7	0.91
Brain	6.46 ± 0.10	0.94	6.00 ± 0.09**	1.04
Cecum	3.75 ± 0.33	0.91	3.97 ± 0.33	0.97
Colon	4.08 ± 0.22	0.37	4.65 ± 0.32	0.36
Duodenum	4.11 ± 0.27	0.58	3.70 ± 0.21	0.73
Eyes	0.31 ± 0.03	0.66	0.30 ± 0.04	0.77
Heart	1.58 ± 0.02	1.20	1.62 ± 0.02	1.32
Ileum	3.27 ± 0.23	0.46	3.26 ± 0.27	0.51
Jejunum	8.36 ± 0.45	0.52	9.35 ± 0.46	0.55
Kidney	4.61 ± 0.16	0.85	4.11 ± 0.08**	1.08
Liver	16.54 ± 0.36	1.25	16.56 ± 0.33	1.40
Lung	2.80 ± 0.07	1.21	2.57 ± 0.04**	1.50
Muscle	87.6 ± 2.8	1.10	95.5 ± 2.9*	1.14
Pancreas	7.65 ± 0.34	1.46	5.85 ± 0.18**	1.26
Pelt	116.0 ± 2.0	0.88	120.3 ± 3.8	0.96
Plasma	1.04 ± 0.06	1.00	1.17 ± 0.04	1.00
RBC	4.15 ± 0.20	1.15	4.31 ± 0.12	1.25
Reproductive tract	3.30 ± 0.19	1.05	2.52 ± 0.09**	1.54
Spleen	0.83 ± 0.03	0.91	0.82 ± 0.02	1.04
Stomach	3.29 ± 0.26	0.65	3.42 ± 0.23	0.71
Total	561.5 ± 18.2	1.01	582.8 ± 16.3	1.08

¹ Values are means ± SEM. *Different from WT, $P < 0.05$; ** $P < 0.01$.

² To convert to μmol , multiply by 0.0153.

³ Calculated to observed mass ratio; calculated values were determined using the model in Figure 1.

pools of Zn, as do those (RBC and liver) shown previously to have 2 pools in humans (3). Notably, the results of Sheline et al. (8) show much greater uptake of tracer by the liver following i.v. administration than in our study where tracer was administered orally. Zn absorption (23%) matched that (22%) determined by Cotzias et al. (9).

The additional Zn pools identified in mice are probably the result of being able to directly sample more tissues. Pool turnover times in mice were ~5 times faster than those in rats (1). Studies in rats showed that the tracer curves of kidneys, spleen, and testes corresponded in shape to 3 previously unidentified pools in humans (1), indicating that Zn kinetics in rodents may assist in interpretation of human data. It is generally considered that refining existing models is more likely to improve prediction rather than inventing new models. Certainly when models do not fit a new set of data (37), those aspects not fitted need to be described before the model is abandoned, because the error may lie with either the original or the new data rather than the model per se. Our understanding of human Zn metabolism and its regulation has been assisted by kinetic studies during normal Zn intake (4,5,38), increased Zn intake where 5 sites were identified (4), and with Zn deficiency (39). However, our knowledge of the roles of specific proteins in these processes is limited. The kinetic results described here on the loss of MT from mice may provide insight into how metabolism is regulated. The approach could be generalized and applied to identify the role of specific proteins in the metabolism of other nutrients.

TABLE 4 Values for fractional rate constants for transfer of Zn from compartment j to compartment i ($L_{i,j}$) in model of Zn kinetics in mice

Parameter ¹	Value (FSD) ²	Description	Parameter ¹	Value (FSD) ²	Description
	h^{-1}			h^{-1}	
L(00,18)	0.003	Loss from skin	L(13,03)	0.010	Slow muscle from fast muscle
L(01,03)	0.050 (0.11)	Plasma from fast muscle	L(14,01)	1.195 (0.33)	Pancreas from plasma (WT)
L(01,05)	0.130	Plasma from fast RBC	L(14,01)	1.531 (0.13)	Pancreas from plasma (MT-/-)
L(01,07)	0.049 (0.13)	Plasma from fast bone	L(17,07)	0.010	Slow bone from fast bone
L(01,08)	0.467 (0.28)	Plasma from fast liver	L(18,01)	1.897 (0.14)	Skin from plasma
L(01,10)	0.541 (0.36)	Plasma from kidney	L(18,19)	0.0007	Fast skin from slow skin
L(01,11)	0.128 (0.14)	Plasma from adrenal, eye, spleen	L(19,18)	0.005	slow skin from fast skin
L(01,14)	0.111 (0.39)	Plasma from pancreas (WT)	L(21,23)	0.026 (0.39)	Stomach tissue from lumen
L(01,14)	0.243 (0.16)	Plasma from pancreas (MT-/-)	L(22,01)	0.001	Reprod. tract from plasma
L(01,18)	0.154 (0.18)	Plasma from skin	L(23,21)	0.005	Lumen from stomach tissue
L(01,22)	0.005	Plasma from reproductive tract	L(24,01)	0.110	Duodenum from plasma
L(01,24)	0.069 (0.30)	Plasma from duodenum	L(24,23)	3.588 (0.19)	Duodenum from stomach
L(01,26)	0.011 (0.15)	Plasma from brain	L(24,33)	0.014 (0.54)	Lumen from duodenal tissue
L(01,34)	0.084 (0.20)	Plasma from jejunum	L(25,36)	0.139 (0.15)	Colon from cecum
L(01,36)	0.013 (0.20)	Plasma from cecum	L(25,42)	0.01	Colon from tissue
L(03,01)	1.549 (0.07)	Muscle from plasma	L(26,01)	0.061 (0.08)	Brain from plasma
L(03,13)	0.005 (0.40)	Fast muscle from slow muscle	L(33,24)	0.040	Tissue from duodenum
L(04,25)	0.476 (0.21)	Colon to feces	L(34,01)	0.237 (0.55)	Jejunum from plasma
L(05,01)	0.156 (0.10)	Fast RBC from plasma	L(34,24)	1.797 (0.20)	Jejunum from duodenum
L(05,06)	0.052 (0.18)	Fast RBC from slow RBC	L(34,37)	0.010	Jejunum from tissue
L(06,05)	0.150	Slow RBC from fast RBC	L(35,34)	0.600 (0.16)	Ileum from jejunum
L(07,01)	1.846 (0.08)	Bone from plasma	L(35,39)	0.002	Ileum from tissue
L(07,17)	0.002	Fast bone from slow bone	L(36,35)	1.049 (0.13)	Cecum from ileum
L(08,01)	5.627 (0.20)	Liver from plasma	L(36,41)	0.015	Cecum from tissue
L(08,09)	0.082 (0.31)	Fast liver from slow liver	L(37,34)	0.017 (0.50)	Tissue from jejunum
L(09,08)	0.054	Slow liver from fast liver	L(39,35)	0.002	Tissue from ileum
L(10,01)	2.044 (0.30)	Kidney from plasma	L(40,01)	0.015 (0.31)	Delay into urine from plasma
L(11,01)	8.42 (0.30)	Adrenal, eye, spleen from plasma	L(41,36)	0.005	Tissue from cecum
L(12,40)	1.	Urine from delay	L(42,25)	0.005	Tissue from colon

¹ Parameters relate to model in Figure 1. Parameter values were the same for both genotypes except for exchange with the pancreas; L(14,1) and L(1,14) differed between WT and MT-null (MT-/-) mice. Delay time, DT (40), before excretion of Zn into urine was 20 h.

² Fractional SD (FSD) are shown for each parameter that was allowed to adjust during the data fitting; all other parameters were fixed.

Zn concentrations in tissues are influenced by age, gender, diet, and genetic background and these factors may explain why Zn concentrations in some tissues in our study varied from values reported for other strains of mice. For example, total hepatic Zn and skeletal muscle Zn concentration measured here were lower than values reported for C57BL/6J mice (10,40,41). However, the total amount of Zn in other tissues, such as the pancreas, was similar to the amount in lean C57BL/6J mice (40).

MT-/- mice. Although feed intake did not differ between groups, MT-/- mice were ~5% heavier at 10 wk old than the WT mice. Whereas a trend toward obesity was reported in 6-wk-old male MT-null mice of mixed genetic background (129/Ola and C57BL/6J) compared with control C57BL/6J mice (42), others (23) reported that MT did not affect body weight when mice of identical background were compared. The variation in body weight that we observed may be a carry-over effect from weaning weights. Duffy et al. (43) reported that the mean weight of pups at weaning from MT-null dams was higher than that of pups from WT dams (strain 129/Sv), but the degree of difference or ratio of gender was not given. We have observed (W. A. House, unpublished data) that the mean body weights of female MT-null and WT 129/Sv mice did not differ significantly when the mice were older (32–39 wk old). We suggest, therefore, that

MT does not have a major role in the regulation of energy utilization in female mice fed a diet containing adequate Zn.

Generally, tissue concentrations of Zn were lower in the MT-null mice than in the WT mice, particularly in the pancreas, which agrees with an earlier report (44). Differences in tissue Zn concentrations of MT-null and WT mice would appear to support one of the suggestions proposed for the function of MT, namely that MT can serve as a transient reservoir for the storage of metals, including Zn (23,45). Whole-body Zn concentration, by contrast, was ~28 $\mu\text{g/g}$ body weight in both groups, suggesting that MT probably does not have a marked effect on Zn balance in nutritionally replete animals. Plasma glucose concentration in MT-/- mice has been reported to be either similar to (42,46) or lower than (47) that in WT mice. The higher values of fasting plasma glucose and insulin that we observed in the MT-/- mice may reflect different responses to stress between the genotypes.

Zn kinetics: MT-/- vs. WT

Whole-body Zn kinetics were used to quantify differences in Zn metabolism between MT-/- and WT mice. In fed, female mice, lack of MT-1 and MT-II did not affect Zn absorption or Zn kinetics in most tissues. However, as observed previously (26,27), lack of MT did alter Zn kinetics in the pancreas. In our study, this

difference between mouse genotypes, explained through modeling, was a 2-fold faster rate of turnover of Zn in the pancreas of MT^{-/-} mice compared with WT mice. We did not observe other differences (Zn tracer in liver, muscle, and skin) that were reported in the food-deprived mice (26). Based on samples collected at 2 time points, Rofe et al. (26) concluded that the MT-null mice secreted more Zn into the intestine via pancreatic, bile, or intestinal secretions than did WT mice. However, it cannot be determined from observations at 2 time points whether the rate of Zn secretion into intestine is higher or rate of removal is altered. Although Zn efflux from the pancreas to the small intestine is considered an important pathway (48–50), we were not able to define this pathway kinetically from either our earlier studies in rats (1) or our current study where tracer was administered orally. Others (5) have included a separate pathway from tissues to the intestine to represent endogenous loss and separate absorption pathways. Interestingly, absorption from the 2 sites in the small intestine, calculated using their (5) parameter values, was similar (~15%) in the fed subjects. Our model simulations for mice indicated that the major Zn loss from pancreas was via plasma. In support of this, endogenous fecal excretion was not reduced after pancreatectomy in control mice (26).

Interpretation: Zn kinetics in the pancreas in the presence and absence of MT

About 1% of the pancreas consists of Islet cells (composed of glucagon-secreting α cells and insulin-secreting β cells) that may contain up to 20 times the amount of Zn found in the other cell type, the acinar cells [see (51)]. About one-third of the Zn in rat Islet cells is associated with insulin (i.e. in the granules) (52). Tracer studies in rats showed that acinar cells take up Zn rapidly and it then turns over in ~24 h whereas Islet cells continue to retain high tracer levels beyond 92 h (51). We were able to identify only a single pancreatic Zn pool from our *in vivo* data and this pool presumably represents the more slowly exchanging Zn in Islet cells. As some investigators (50) reported that Islets in mice, in contrast to rats (53), do not contain MT, the difference we observed in pancreatic Zn kinetics between WT and MT^{-/-} mice may likely be due to Zn kinetics in the acinar cells (47,54). However, others have found similar levels of MT in mice and rat Islets (47). We could speculate that the difference in Zn mass in pancreas of WT and MT^{-/-} mice is the proportion of Zn bound to MT (23%) in the fed female mice. However, with the existence of Zn transporters, including one specific to the pancreas (55–57), this interpretation may be too simplistic. Namely, MT may facilitate movement of Zn into a specific cellular pool, enzyme, or storage form so that the difference in kinetics represents these other forms of Zn rather than MT-bound Zn. Experimental measurements of the location of Zn tracer in pancreas ~15–45 h after gavage may indicate the form or location of Zn resulting from the presence of MT. In our model, the pancreatic pool, therefore, represents Zn in both acinar and Islet cells.

Our study provides baseline values for Zn kinetics in fed mice. These baseline values can be used to evaluate roles of specific proteins in Zn metabolism *in vivo*. By comparing Zn kinetics in MT- knockout and WT control mice with the same genetic background, we have confirmed that the pancreas is the primary tissue affected by the absence of MT-I and MT-II. Under replete dietary conditions, Zn in the pancreas of MT-null mice turns over twice as fast as Zn in WT mice. More detailed studies are required to determine how lack of MT alters Zn metabolism within the pancreas. In addition, an expansion of the Zn model to include intracellular metabolism and movement of Zn and MT within Islet and acinar cells (58) and parallel modeling of the dynamics of

MT and Zn metabolism will further unravel the roles of these compounds.

Literature Cited

- House WA, Wastney ME. Compartmental analysis of zinc kinetics in mature male rats. *Am J Physiol.* 1997;273:R1117–25.
- Wastney ME, House WA, Barnes RM, Siva Subramanian KN. Kinetics of zinc metabolism: variation with diet, genetics and disease. *J Nutr.* 2000;130:S1355–9.
- Foster DM, Aamodt RL, Henkin RI, Berman M. Zinc metabolism in humans: a kinetic model. *Am J Physiol.* 1979;237:R340–9.
- Wastney ME, Aamodt RL, Rumble WF, Henkin RI. Kinetic analysis of zinc metabolism and its regulation in normal humans. *Am J Physiol.* 1986;251:R398–408.
- Miller LV, Krebs NF, Hambidge KM. Development of a compartmental model of human zinc metabolism: identifiability and multiple studies analyses. *Am J Physiol Regul Integr Comp Physiol.* 2000;279:R1671–84.
- Dunn MA, Cousins RJ. Kinetics of zinc metabolism in the rat: effect of dibutyl cAMP. *Am J Physiol.* 1989;256:E420–30.
- Serfass RE, Fang Y, Wastney ME. Zinc kinetics in weaned piglets fed marginal zinc intake: compartmental analysis of stable isotopic data. *J Trace Elem Exp Med.* 1996;9:73–86.
- Sheline GE, Chaikoff IL, Jones HB, Montgomery ML. Studies on the metabolism of zinc with the aid of its radioactive isotope. II. The distribution of administered radioactive zinc in the tissues of mice and dogs. *J Biol Chem.* 1943;149:139–51.
- Cotzias GC, Borg DC, Selleck B. Specificity of zinc pathway through the body: turnover of Zn⁶⁵ in the mouse. *Am J Physiol.* 1962;202:359–63.
- Reis BL, Keen CL, Lonnerdal B, LS Hurley. Mineral composition and zinc metabolism in female mice of varying age and reproductive status. *J Nutr.* 1988;118:349–61.
- He LS, Yan XS, Wu DC. Age-dependent variation of zinc-65 metabolism in LACA mice. *Int J Radiat Biol.* 1991;60:907–16.
- McCall KA, Huang C, Fierke CA. Function and mechanism of zinc metalloenzymes. *J Nutr.* 2000;130:S1437–46.
- Liuzzi JP, Bobo JA, Lichten LA, Samuelson DA, Cousins RJ. Responsive transporter genes within the murine intestinal-pancreatic axis form a basis of zinc homeostasis. *Proc Natl Acad Sci USA.* 2004;101:14355–60.
- Cousins RJ, Liuzzi JP, Lichten LA. Mammalian zinc transport, trafficking, and signals. *J Biol Chem.* 2006;281:24085–9.
- Sekler I, Sensi SL, Hershinkel M, Silverman WF. Mechanism and regulation of cellular zinc transport. *Mol Med.* 2007;13:337–43.
- Klaassen CD, Liu J, Choudhuri S. Metallothionein: an intracellular protein to protect against cadmium toxicity. *Annu Rev Pharmacol Toxicol.* 1999;39:267–94.
- Palmiter RD. Protection against zinc toxicity by metallothionein and zinc transporter 1. *Proc Natl Acad Sci USA.* 2004;101:4918–23.
- Kelly EJ, Quaife CJ, Froelick GJ, Palmiter RD. Metallothionein I and II protect against zinc deficiency and zinc toxicity in mice. *J Nutr.* 1996;126:1782–90.
- Tran CD, Bulter RN, Philcox JC, Rofe AM, Howarth GS, Coyle P. Regional distribution of metallothionein and zinc in the mouse gut. *Biol Trace Elem Res.* 1998;63:239–51.
- Bremner I, Beattie JH. Metallothionein and the trace minerals. *Annu Rev Nutr.* 1990;10:63–83.
- Michalska AE, Choo KHA. Targeting and germ-line transmission of a null mutation at the metallothionein I and II loci in mouse. *Proc Natl Acad Sci USA.* 1993;90:8088–92.
- Masters BA, Kelly EJ, Quaife CJ, Brinster RL, Palmiter RD. Targeted disruption of metallothionein I and II genes increases sensitivity to cadmium. *Proc Natl Acad Sci USA.* 1994;91:584–8.
- Palmiter RD. The elusive function of metallothioneins. *Proc Natl Acad Sci USA.* 1998;95:8428–30.
- Davis S, Cousins R. Metallothionein expression in animals: a physiological perspective on function. *J Nutr.* 2000;130:1085–8.
- Coyle P, Philcox JC, Carey LC, Rofe AM. Metallothionein: the multipurpose protein. *Cell Mol Life Sci.* 2002;59:627–47.

26. Rofe AM, Winters N, Hinskens B, Philcox JC, Coyle P. The role of the pancreas in intestinal zinc secretion in metallothionein-null mice. *Pancreas*. 1999;19:69–75.
27. Coyle P, Philcox JC, Rofe AM. Metallothionein-null mice absorb less Zn from an egg-white diet, but a similar amount from solutions, although with altered intertissue Zn distribution. *J Nutr*. 1999;129:372–9.
28. Iszard MB, Liu J, Liu Y, Dalton T, Andrews GK, Palmiter RD, Klassen CD. Characterization of metallothionein-I-transgenic mice. *Toxicol Appl Pharmacol*. 1995;133:305–12.
29. Onosaka S, Min K-S, Fujita Y, Tanaka K, Iguchi S, Okada Y. High concentration of pancreatic metallothionein in normal mice. *Toxicology*. 1988;50:27–35.
30. Jacob C, Maret W, Vallee BL. Control of zinc transfer between thionein, metallothionein, and zinc proteins. *Proc Natl Acad Sci USA*. 1998;95:3489–94.
31. Cherian MG. Studies on the synthesis and metabolism of zinc-thionein in rats. *J Nutr*. 1977;107:965–72.
32. Reeves PG, Nielsen FH, Fahey GC Jr. AIN-93 purified diets for laboratory rodents: final report of the American Institute of Nutrition ad hoc writing committee on the reformulation of the AIN-76A rodent diet. *J Nutr*. 1993;123:1939–51.
33. Eaton DL, Toal BF. Evaluation of the Cd/hemoglobin affinity assay for the rapid determination of metallothionein in biological tissues. *Toxicol Appl Pharmacol*. 1982;66:134–42.
34. Welch R, House W. Absorption of radiocadmium and radioselenium by rats fed intrinsically and extrinsically labeled lettuce leaves. *Nutr Rep Int*. 1980;21:135–45.
35. Greif P, Wastney M, Linares O, Boston R. Balancing needs, efficiency, and functionality in the provision of modeling software: a perspective of the NIH WinSAAM project. *Adv Exp Med Biol*. 1998;445:3–20.
36. Wastney ME, Patterson BH, Linares OA, Greif PC, Boston RC. Investigating biological systems using modeling: strategies and software. New York: Academic Press; 1998.
37. Miller LV, Krebs NF, Hambidge KM. Human zinc metabolism: advances in the modeling of stable isotope data. *Adv Exp Med Biol*. 1998;445:253–69.
38. Lowe NM, Shames DM, Woodhouse LR, et al. A compartmental model of zinc metabolism in healthy women using oral and intravenous stable isotope tracers. *Am J Clin Nutr*. 1997;65:1810–9.
39. King JC, Shames DM, Lowe NM, et al. Effect of acute zinc depletion on zinc homeostasis and plasma zinc kinetics in men. *Am J Clin Nutr*. 2001;74:116–24.
40. Kennedy M, Failla M. Zinc metabolism in genetically obese (ob/ob) mice. *J Nutr*. 1987;117:886–93.
41. Kennedy M, Failla M, Smith JJ. Influence of genetic obesity on tissue concentrations of zinc, copper, manganese and iron in mice. *J Nutr*. 1986;116:1432–41.
42. Beattie J, Wood A, Newman A, et al. Obesity and hyperleptinemia in metallothionein (-I and -II) null mice. *Proc Natl Acad Sci USA*. 1998;95:358–63.
43. Duffy J, Baines D, Keen C, Daston G. Developmental outcome of metallothionein-null mice fed various levels of zinc during gestation. *Teratology*. 1997;55:54.
44. Liu J, Liu Y, Michalska AE, Choo KHA, Klaasen CD. Distribution and retention of cadmium in metallothionein I and II null mice. *Toxicol Appl Pharmacol*. 1996;136:260–8.
45. Bremner I. Nutritional and physiologic significance of metallothionein. *Methods Enzymol*. 1991;205:25–35.
46. Apostolova M, Choo K, Michalska A, Tohyama C. Analysis of the possible protective role of metallothionein in streptozotocin-induced diabetes using metallothionein-null mice. *J Trace Elem Med Biol*. 1997;11:1–7.
47. Laychock SG, Duzen J, Simpkins CO. Metallothionein induction in islets of Langerhans and insulinoma cells. *Mol Cell Endocrinol*. 2000;165:179–87.
48. McClain C. The pancreas and zinc homeostasis. *J Lab Clin Med*. 1990;116:275–6.
49. Finley F, Johnson P, Reeves P, Vanderpool R, Briske-Anderson M. Effect of bile/pancreatic secretions on absorption of radioactive or stable zinc: in vivo and in vitro studies. *Biol Trace Elem Res*. 1994;42:81–96.
50. De Lisle RC, Sarras MP Jr, Hidalgo J, Andrews GK. Metallothionein is a component of exocrine pancreas secretion: implications for zinc homeostasis. *Am J Physiol*. 1996;271:C1103–10.
51. McIsaac R. The distribution of zinc-65 in the rat pancreas. *Endocrinology*. 1955;57:571–9.
52. Figlewicz D, Formby B, Hodgson A, Schmid F, Grodsky G. Kinetics of ⁶⁵Zn uptake and distribution in fractions from cultured rat Islets of Langerhans. *Diabetes*. 1980;29:767–73.
53. Andrews GK, Kage K, Palmiter-Thomas P, Sarras MP Jr. Metal ions induce expression of metallothionein in pancreatic exocrine and endocrine cells. *Pancreas*. 1990;5:548–54.
54. Minami T, Schimizu M, Tanaka H, Okazaki Y, Cherian M. Metallothionein does not protect mouse endocrine cells from damage induced by alloxan injection. *Toxicology*. 1999;132:33–41.
55. Kambe T, Narita H, Yamaguchi-Iwai Y, et al. Cloning and characterization of a novel mammalian zinc transporter, zinc transporter 5, abundantly expressed in pancreatic beta cells. *J Biol Chem*. 2002;277:19049–55.
56. Chimienti F, Devergnas S, Favier A, Seve M. Identification and cloning of a beta-cell-specific zinc transporter, ZnT-8, localized into insulin secretory granules. *Diabetes*. 2004;53:2330–7.
57. Chimienti F, Devergnas S, Pattou F, et al. In vivo expression and functional characterization of the zinc transporter ZnT8 in glucose-induced insulin secretion. *J Cell Sci*. 2006;119:4199–206.
58. Gyulkhandanyan AV, Lee SC, Bikopoulos G, Dai F, Wheeler MB. The Zn²⁺-transporting pathways in pancreatic beta-cells: a role for the L-type voltage-gated Ca²⁺ channel. *J Biol Chem*. 2006;281:9361–72.